



Published in final edited form as:

Biochem Biophys Res Commun. 2010 December 3; 403(1): 108–113. doi:10.1016/j.bbrc.2010.10.128.

Intercellular transfer regulation of the paracrine activity of GPI-anchored Cripto-1 as a Nodal co-receptor

Kazuhide Watanabe^{a,b} and David S. Salomon^{a,*}

^aMammary Biology & Tumorigenesis Laboratory, Center for Cancer Research, National Cancer Institute, National Institutes of Health, Bethesda, MD 20892

^bDepartment of Biological Chemistry, School of Medicine, University of California, Irvine, CA 92697

Abstract

Cripto-1 (CR-1) is a glycosylphosphatidylinositol-anchored glycoprotein which acts as an obligate co-receptor of a TGF β family ligand, Nodal. Previous studies have demonstrated that CR-1 functions in a paracrine fashion by a cellular mechanism which has not been fully described. This paracrine activity was observed only when CR-1 was expressed as a membrane-bound form and was abolished when CR-1 was expressed in a soluble form. In the current study, we found that there were few biochemical differences in posttranslational modifications between membrane-anchored and soluble forms of CR-1. Flow cytometric analysis revealed an intercellular transfer of the membrane-bound form of CR-1 between cells. CR-1-expressing cells formed unique membrane extensions, generated more membrane fragments than control cells, and exhibited enhanced cellular adhesion. Thus, expression of CR-1 may alter the physiochemical properties of the plasma membrane resulting in an enhancement of intercellular transfer of cellular signaling components which may account for the paracrine activity of CR-1.

Keywords

Cripto-1; GPI-anchored protein; Intercellular transfer; Nodal

Introduction

Nodal signaling is one of the essential signaling pathways during vertebrate development [1]. Nodal belongs to the transforming growth factor β (TGF β) family of ligands and shares its type I and type II receptors and downstream signaling mediators (Smad2/3 and Smad4) with other TGF β family ligands, such as TGF β and Activins. However, unlike TGF β or Activins, Nodal requires EGF-CFC proteins as co-receptors to induce downstream signaling events. Thus, EGF-CFC proteins including mammalian Cripto-1 (CR-1) and Cryptic are also essential for development [2]. Previous studies have suggested that epidermal growth factor-Cripto-1/FRL-1/Cryptic (EGF-CFC) proteins function not only in a cell-autonomous manner but also in non-cell-autonomous manner *in vitro* as well as *in vivo* [3;4;5]. Our previous study suggested that CR-1 functions as a Nodal co-receptor in a cell-autonomous manner as

*Corresponding author: David S. Salomon, PhD, Bldg37 Rm1118B 37 Convent Drive, Bethesda, MD 20892. TEL/FAX: +1 301 402 8656, salomond@mail.nih.gov.

Publisher's Disclaimer: This is a PDF file of an unedited manuscript that has been accepted for publication. As a service to our customers we are providing this early version of the manuscript. The manuscript will undergo copyediting, typesetting, and review of the resulting proof before it is published in its final citable form. Please note that during the production process errors may be discovered which could affect the content, and all legal disclaimers that apply to the journal pertain.

well as in non-cell-autonomous manner only when it was expressed in membrane-attached forms either via glycosylphosphatidylinositol (GPI)-anchor or via a transmembrane domain. In contrast, when CR-1 was expressed as a COOH-terminal truncated soluble form or when Cryptic was mutated in its COOH-terminal region, the activity of these EGF-CFC proteins to assist Nodal signaling activity was completely lost [5;6]. This suggests that a membrane-anchor is required for CR-1 or Cryptic to function as a Nodal co-receptor.

However, it was unclear how membrane-anchored CR-1 or Cryptic could function in a paracrine fashion. We had proposed two hypotheses in our previous publication to explain this paradoxical phenomenon [5]. First, specific post-translational modifications such as glycosylation which is required for proper function of CR-1 may only occur when CR-1 is expressed as membrane-anchored forms, where a GPI-anchored form of CR-1 functions in a paracrine fashion through a “shedding” mechanism by GPI-phospholipase D, which has been previously described [7]. Alternatively, the membrane-anchorage *per se* is required for CR-1 to function and a membrane-form of protein could be transferred intercellularly through an unknown mechanism.

To test these possibilities, we assessed if there were biochemical differences in posttranslational modifications between the GPI-anchored and soluble forms of CR-1 that would indicate any alterations between these forms. We also ascertained if there was any possible intercellular transfer of the membrane forms of CR-1 by FACS analysis. We found that intercellular transfer of GPI-anchored CR-1 is a likely mechanism rather than altered posttranslational modifications for regulating the paracrine activity of CR-1 as a Nodal co-receptor.

Materials and methods

Cell culture

COS-7, 293T, and rat IEC6 intestinal cells were purchased from ATCC (Manassas, VA). IEC6 clones were generated by G418 selection and limiting dilution to clonal density after transfection of an empty vector (EV) or a CR-1 expression vector [7]. COS-7 and 293T cells were cultured in Dulbecco's modified Eagles medium (DMEM) supplemented with 10% fetal bovine serum (FBS). IEC6 cells were cultured in DMEM supplemented with 10% FBS and 0.1-unit/mL insulin.

Expression vectors

Wild-type (CR1WT), soluble (CR1S161), and transmembrane (CR1TM) forms of CR-1 expression vectors were previously described [7]. Tobacco Etch Virus (TEV) protease-cleavable constructs were generated based on the NH₂-terminal 3xFlag Cripto-1 constructs [8]. EcoRV site was introduced into the corresponding nucleotide sequence of four amino acid upstream of Serine 161 by site-directed mutagenesis and synthesized oligo DNA which encodes for a TEV cleavage sequence followed by a V5 epitope was inserted into the generated EcoRV site.

Immunofluorescence

Cells grown in chamber slides were washed with phosphate-buffered saline (PBS) and fixed in 4% paraformaldehyde. Depending on the experiment, cells were permeabilized with 0.2% Triton X-100. After blocking, CR-1 was labeled with 5 µg/mL of anti-human CR-1 mouse monoclonal antibody (MAB2771, R&D Systems, Minneapolis, MN) and detected with Alexa Fluor 488-conjugated anti-mouse secondary antibody (Invitrogen). Plasma membrane and actin cytoskeleton were detected with 5 µg/mL of wheat germ agglutinin (WGA)- or with 5 unit/mL of phalloidin-Alexa Fluor 594 conjugate (Invitrogen), respectively. Images were

obtained using a Zeiss LSM 510 NLO Meta confocal system (Carl Zeiss, Göttingen, Germany) with an Axiovert 200M inverted microscope equipped with a 63× NA1.4 Plan-Apochromat oil immersion objective lens.

Dual luciferase assay

Dual luciferase assays were performed as described previously with 293T cells which had been transfected with an optimized amount of expression vectors ((n2)7-Luc, TK-renilla, mFast-1, mNodal, ALK4-HA, and CR-1 mutants). After 24 h of transfection, dual luciferase assays were carried out using a kit provided by Promega (Madison, WI) according to the manufacturer's instructions.

TEV protease treatment and Western blot analysis

TEV-cleavable, Flag-tagged CR-1 proteins were purified from transiently transfected 293T cells using anti-Flag M2 agarose and 3x Flag peptide (Sigma-Aldrich, St. Louis, MO) and treated with AcTEV protease (Invitrogen, Carlsbad, CA) according to the manufacturer's instruction. Digested proteins were separated on 4-20% SDS-PAGE gels (Invitrogen) and were detected with an anti-Cripto (V17, Santa Cruz Biotechnology, Santa Cruz, CA) or an anti-V5 (Invitrogen) antibody.

FACS analysis

FACS detection of cell-surface CR-1 was performed using anti-human CR-1 Phycoerythrin (PE)-conjugated mouse monoclonal antibody (FAB2772P, R&D Systems) as described previously [5]. Cells that had been labeled with CellTracker green CMFDA (Invitrogen) were excluded from analysis (Fig. 2A and B) and only non-labeled populations were analyzed for the cell-surface CR-1 expression.

Adhesion assay

To measure cell adhesion, IEC6 clones were plated at a density of 100,000 cells/mL. Cells were allowed to adhere for 45 min at 37°C. Non-adherent cells were removed by washing with PBS, and the remaining cells were fixed with 70% ethanol and total and flattened cells were counted manually.

Results and Discussion

We have previously shown that the GPI-linked and soluble forms of CR-1 exhibit different mobilities on SDS-PAGE and that the GPI-linked form migrates significantly slower than the soluble form even though the amino acid sequences of mature proteins are identical [5] (Fig. 1A and B). We demonstrated that this difference in electrophoretic mobility was still apparent even after treatment of GPI-linked form with phosphatidylinositol-phospholipase C (PI-PLC) (please see Fig. 7D in [5]) suggesting that this difference was not due to the lipid modification and was possibly due to the additional modifications which might only occur when proteins were expressed as membrane-anchored forms. However, since PI-PLC cleaves between phosphatidylinositol and fatty acid (please see Fig. 7A in [7]), the GPI moiety should still exist even after PI-PLC treatment and it is possible that the difference in mobility was simply because of the residual GPI moiety. To test the possible difference in post-translational modifications between GPI-anchored and soluble forms, we introduced TEV protease cleavage sequence at the four amino acid upstream of Serine 161 which we identified as an omega-site in the GPI-anchored form [5] and which is the last amino acid in the soluble form (Fig. 1A). These artificial proteins behaved similarly to the corresponding non-tagged forms as assessed by subcellular localization and by Nodal reporter assay (Fig. 1B and C). GPI-linked forms were expressed in the membrane as well as in the ER-Golgi

network and soluble forms were detected only in the ER-Golgi (Fig. 1B). Both of the GPI-linked forms were able to activate the Nodal signaling whereas this activity was completely lost in the soluble forms as described previously (Fig. 1C) [5]. By using these TEV protease cleavable constructs, we were able to compare the size of the two forms of the protein upon exclusion of GPI moiety. If the GPI-anchored form undergoes different post-translational modifications which were absent from soluble form, mobility of these two proteins after TEV cleavage should be different. However, TEV protease treatment of the GPI-anchored form produced a major 26-kD band which was almost identical in size to that of the soluble form that was also treated with TEV protease (Fig. 1D). The faint 30-kD band in the TEV-treated, GPI-anchored form was likely due to incomplete digestion by TEV protease. Detection with V5 epitope which was introduced at the NH₂-terminus of the TEV cleavage site resulted in disappearance of the major forms and appearance of 5-10-kDa peptide from the GPI-anchored form which corresponds to the COOH-terminal fragments containing the GPI moiety (Fig. 1B). Thus, the additional post-transcriptional modifications which only occur in the GPI-form are unlikely even though we could not entirely exclude the possibility of undetectable minor modifications. This finding is also supported by the mass-spectrometric LC-MS/MS analysis of the “shed” GPI-anchored CR-1 ([7], unpublished data). We did not observe, at least in the glycosylation status, any significant differences when compared to a similar analysis of soluble Fc-fusion form of CR-1 except for the COOH-terminal GPI modification [9].

To ascertain if intercellular transfer of membrane-forms of CR-1 might occur, we performed co-culture experiments of Celltracker-labeled CR-1 expressing 293T cells and non-labeled, CR-1-negative 293T cells, followed by cell-surface detection of CR-1 protein by FACS analysis (Fig. 2A). 293T cells were transfected with EV or CR1WT expression vectors and subsequently labeled with the Celltracker reagent. Labeling efficiency with the Celltracker marker was 100% for at least 5 days (data not shown). The transfected, labeled 293T cells were then cultured for 24 hours with non-labeled, wild-type 293T cells and CR-1 expression was determined by cell-surface staining of CR-1 with a PE-labeled anti-CR-1 monoclonal antibody followed by FACS. To exclude the transfected, Celltracker-labeled 293T cells from the analysis, we first gated out the Celltracker-positive population which showed a clearly distinct peak from the Celltracker-negative population (Fig. 2B, peak B and A, respectively). Even though the unlabeled population did not express endogenous nor exogenous CR-1 transcript, cell-surface CR-1 expression of the 293T cells which had been co-cultured with CR1WT-transfected, Celltracker-positive 293T cells was significantly increased compared to the control 293T cells which had been co-cultured with the EV-transfected, Celltracker-positive 293T cells assessed by FACS analysis using a PE-labeled anti-CR-1 monoclonal antibody (7.6 ± 1.8 -fold increase in the median fluorescence, $n=3$, Fig. 2C peak I and II). This suggested that the CR-1 protein was intercellularly transferred from cell to cell while retaining membrane-anchorage. To assess if the transferred CR-1 was still attached to the membrane via GPI-anchor, we treated the co-cultured cells with PI-PLC and the cell-surface expression of CR-1 in the non-labeled population was then analyzed (Fig. 2D). PI-PLC treatment almost completely abolished the cell-surface reactivity of CR-1 in this population, suggesting that CR-1 protein was transferred as a GPI-anchored form. This intercellular transfer phenomenon was not unique to 293T cells since it was also observed when COS-7 cells were either a recipient or a donor, even though the 293T cells showed a more efficient transfer as a donor, suggesting that transfer efficiency varies between cell types (Fig. 2E). As the paracrine activity of CR-1 was still retained when it was expressed as a transmembrane form (data not shown)[5;7], the transmembrane form of CR-1, CR1TM, was also found to be intercellularly transferred from cell to cell (Fig. 2F). Collectively, these results suggest that CR-1 can be transferred intercellularly as a membrane protein. In fact, careful re-examination of our previous data revealed two clearly distinct peaks of cell-surface CR-1 expression following transient transfection and subsequent FACS analysis of

293T or COS-7 [5;8;10] (Fig. 2C peak III and IV). We have described, in these previous studies, that these two populations may represent high and low expressing populations, respectively. However, it is more likely that exogenously expressed CR-1 was transferred to the non-transfected cells because the transfection efficiency was not 100% in these studies [5] and because the 293T or COS7 cells do not express endogenous CR-1 [3;5].

The results of the FACS analysis led us to carefully re-examine the subcellular localization of CR-1 by immunofluorescence and confocal microscopy. Unlike FACS analysis, we failed to see transferred CR-1 in non-transfected populations following co-culture with donor CR-1 expressing cells by immunofluorescent analysis, probably because of the different sensitivities between these two assays. In fact, the difference of peak intensities in FACS analysis between the donor cells and recipient cells after transfer was ~50 fold (Fig. 2C peak II and IV). Careful analysis of the subcellular localization of CR-1 revealed that CR-1-expressing COS7 or 293T cells showed unique membrane extensions that were rarely seen in the untransfected cells and that CR-1 was localized in these membrane extensions up to the very end of the tips (Fig.3A and B). These membrane extensions were frequently found to form cell to cell contacts (Fig.3 A and B, arrows). Formation of these membrane extensions was more apparent in the cells that were expressing transmembrane form of CR-1 showing neuronal-like projections with numerous fine processes in some cases (Fig. 3B). This unique morphological appearance was never observed in cells expressing soluble forms of CR-1 (data not shown). Although we have not fully characterized the identity of these membrane extensions, these structures may be filopodia or neurite-like structures. Alternatively, expression of CR-1 on the membrane may increase the local adhesiveness of the membrane such that these process-like structures are created as a consequence of cellular movement. To support the latter possibility, more process-like structures as well as possible membrane fragments were observed in the cell-free area on the surface of the plastic plates in the CR1WT- or CR1TM-transfected 293T cells as compared to the EV-transfected 293T control cells (Fig. 3C, arrows). In addition, three-dimensional imaging revealed that CR-1 is located at the attachment surface at the edge of the cell border (Fig. 3D, arrows). These observations suggest the possibility that expression of CR-1 may affect the physiochemical properties of plasma membrane by increasing the adhesiveness of the membrane. To determine if expression of CR-1 affects the adhesiveness of cells, we established stable clones for EV- and CR1WT-transduced cells from a normal rat intestinal epithelial cell line, IEC6. There was no significant difference in cell proliferation among the clones (data not shown). CR-1-expressing IEC6 clones adhered to the plastic plates more quickly and efficiently than control clones (Fig. 3E), suggesting that CR-1 expression may enhance the cell to matrix adhesion and may trigger signaling pathways possibly involving integrins which can cause morphological changes of cells [11].

Intercellular transfer of cellular components has been demonstrated in several different systems (summarized in [12]). For example, this phenomenon is commonly observed in the immune system [12] but it has also been reported in epithelial cells including tumor cells [13;14;15]. Intercellular transfer of membrane components, including GPI-anchored proteins, has also been demonstrated [16]. Intercellular transfer of membrane proteins can be achieved either by vesicular mechanisms [17] or by direct cell-to-cell contact [18]. Transport of exosomes between cells can be easily observed by real-time imaging of cultured cells (movie1). Here we propose a novel model for modulating the paracrine activity of membrane-bound CR-1. Previous studies have clearly demonstrated that CR-1 can act in a paracrine manner [3;4;5]. Our previous data also demonstrates that CR-1 has to be expressed in a membrane-anchored form to function *in cis* (autocrine) as well as *in trans* (paracrine) [5]. However, the mechanism which modulates paracrine function of membrane-bound CR-1 has remained elusive. The present findings strongly suggest that intercellular transfer of membrane-bound CR-1 may be involved in the paracrine action of CR-1. Even though a

relatively low amount of CR-1 proteins can be transferred to CR-1 non-expressing cells (~1/50 in fluorescence intensity by FACS), this amount may be enough to induce Nodal signaling since low concentrations of CR-1 can modulate Nodal-dependent Smad2 phosphorylation and Smad-dependent reporter activation [5]. In addition, expression of CR-1 can enhance the cell to cell contacts as well as the cell to matrix adhesion, which may result in the enhancement of intercellular transfer of cellular components. This effect of CR-1 on the physiochemical properties of the plasma membrane may also relate to the ability of CR-1 to promote cell motility and invasion [11;19].

Research Highlights

- Membrane-anchorage of Cripto-1 is required for its paracrine activity as a Nodal co-receptor
- Cripto-1 can be intercellularly transferred as a membrane protein
- Expression of Cripto-1 alters physiochemical property of plasma membrane and enhances intercellular transfer of membrane components

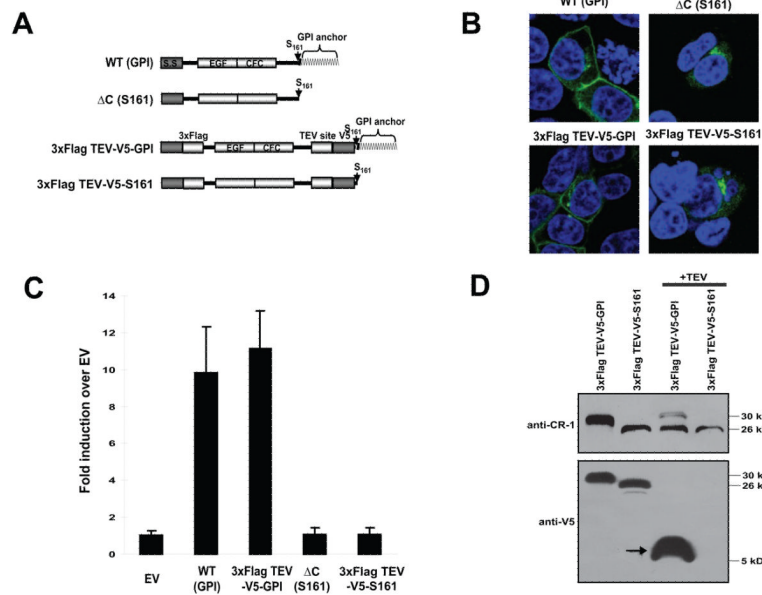
Supplementary Material

Refer to Web version on PubMed Central for supplementary material.

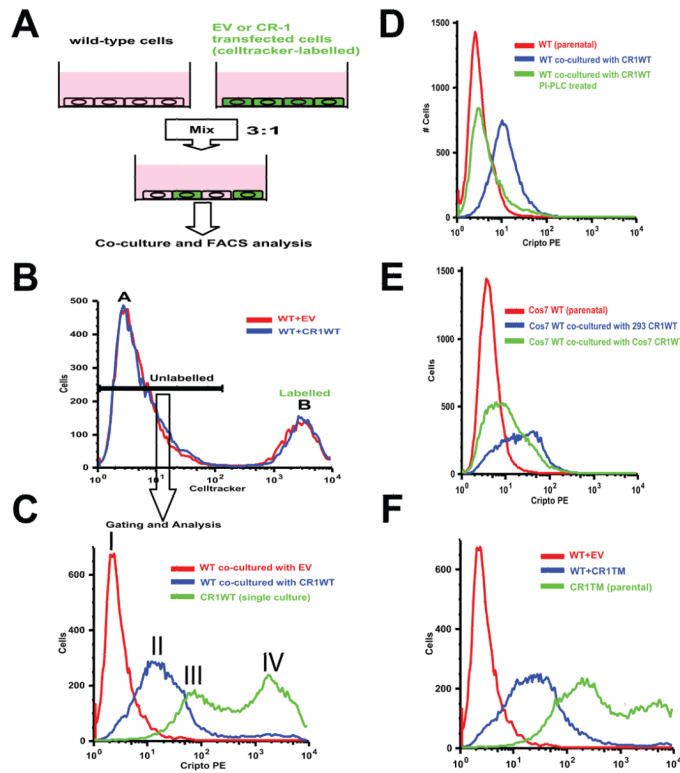
References

1. Shen MM. Nodal signaling: developmental roles and regulation. *Development*. 2007; 134:1023–34. [PubMed: 17287255]
2. Salomon DS, Bianco C, Ebert AD, Khan NI, De Santis M, Normanno N, Wechselberger C, Seno M, Williams K, Sanicola M, Foley S, Gullick WJ, Persico G. The EGF-CFC family: novel epidermal growth factor-related proteins in development and cancer. *Endocr Relat Cancer*. 2000; 7:199–226. [PubMed: 11174844]
3. Yan YT, Liu JJ, Luo Y, E C, Haltiwanger RS, Abate-Shen C, Shen MM. Dual roles of Cripto as a ligand and coreceptor in the nodal signaling pathway. *Mol Cell Biol*. 2002; 22:4439–49. [PubMed: 12052855]
4. Chu J, Ding J, Jeays-Ward K, Price SM, Placzek M, Shen MM. Non-cell-autonomous role for Cripto in axial midline formation during vertebrate embryogenesis. *Development*. 2005; 132:5539–51. [PubMed: 16291788]
5. Watanabe K, Hamada S, Bianco C, Mancino M, Nagaoka T, Gonzales M, Bailly V, Strizzi L, Salomon DS. Requirement of glycosylphosphatidylinositol anchor of Cripto-1 for trans activity as a Nodal co-receptor. *J Biol Chem*. 2007; 282:35772–86. [PubMed: 17925387]
6. Bamford RN, Roessler E, Burdine RD, Saplakoglu U, dela Cruz J, Splitt M, Goodship JA, Towbin J, Bowers P, Ferrero GB, Marino B, Schier AF, Shen MM, Muenke M, Casey B. Loss-of-function mutations in the EGF-CFC gene CFC1 are associated with human left-right laterality defects. *Nat Genet*. 2000; 26:365–9. [PubMed: 11062482]
7. Watanabe K, Bianco C, Strizzi L, Hamada S, Mancino M, Bailly V, Mo W, Wen D, Miatkowski K, Gonzales M, Sanicola M, Seno M, Salomon DS. Growth factor induction of Cripto-1 shedding by glycosylphosphatidylinositolphospholipase D and enhancement of endothelial cell migration. *J Biol Chem*. 2007; 282:31643–55. [PubMed: 17720976]
8. Watanabe K, Nagaoka T, Lee JM, Bianco C, Gonzales M, Castro NP, Rangel MC, Sakamoto K, Sun Y, Callahan R, Salomon DS. Enhancement of Notch receptor maturation and signaling sensitivity by Cripto-1. *J Cell Biol*. 2009; 187:343–53. [PubMed: 19948478]
9. Schiffer SG, Foley S, Kaffashan A, Hronowski X, Zichittella AE, Yeo CY, Miatkowski K, Adkins HB, Damon B, Whitman M, Salomon D, Sanicola M, Williams KP. Fucosylation of Cripto is required for its ability to facilitate nodal signaling. *J Biol Chem*. 2001; 276:37769–78. [PubMed: 11500501]

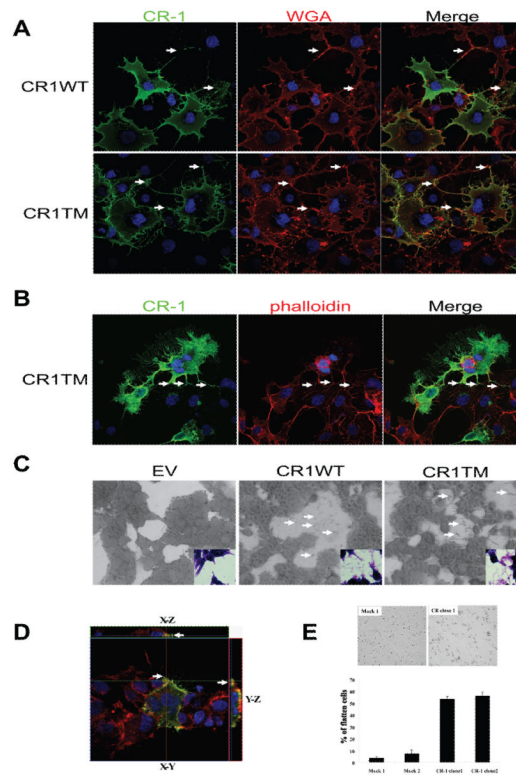
10. Watanabe K, Nagaoka T, Strizzi L, Mancino M, Gonzales M, Bianco C, Salomon DS. Characterization of the glycosylphosphatidylinositol-anchor signal sequence of human Cryptic with a hydrophilic extension. *Biochim Biophys Acta*. 2008; 1778:2671–81. [PubMed: 18930707]
11. Strizzi L, Bianco C, Normanno N, Seno M, Wechselberger C, Wallace-Jones B, Khan NI, Hirota M, Sun Y, Sanicola M, Salomon DS. Epithelial mesenchymal transition is a characteristic of hyperplasias and tumors in mammary gland from MMTV-Cripto-1 transgenic mice. *J Cell Physiol*. 2004; 201:266–76. [PubMed: 15334661]
12. Ahmed KA, Xiang J. Mechanisms of cellular communication through intercellular protein transfer. *J Cell Mol Med*. Jan 11.2010 Epub ahead of print.
13. Niu X, Gupta K, Yang JT, Shablott MJ, Levchenko A. Physical transfer of membrane and cytoplasmic components as a general mechanism of cell-cell communication. *J Cell Sci*. 2009; 122:600–10. [PubMed: 19208767]
14. Levchenko A, Mehta BM, Niu X, Kang G, Villafania L, Way D, Polycarpe D, Sadelain M, Larson SM. Intercellular transfer of P-glycoprotein mediates acquired multidrug resistance in tumor cells. *Proc Natl Acad Sci U S A*. 2005; 102:1933–8. [PubMed: 15671173]
15. Al-Nedawi K, Meehan B, Micallef J, Lhotak V, May L, Guha A, Rak J. Intercellular transfer of the oncogenic receptor EGFRvIII by microvesicles derived from tumour cells. *Nat Cell Biol*. 2008; 10:619–24. [PubMed: 18425114]
16. Anderson SM, Yu G, Giattina M, Miller JL. Intercellular transfer of a glycosylphosphatidylinositol (GPI)-linked protein: release and uptake of CD4-GPI from recombinant adeno-associated virus-transduced HeLa cells. *Proc Natl Acad Sci U S A*. 1996; 93:5894–8. [PubMed: 8650189]
17. Simons M, Raposo G. Exosomes--vesicular carriers for intercellular communication. *Curr Opin Cell Biol*. 2009; 21:575–81. [PubMed: 19442504]
18. Gerdes HH, Carvalho RN. Intercellular transfer mediated by tunneling nanotubes. *Curr Opin Cell Biol*. 2008; 20:470–5. [PubMed: 18456488]
19. Bianco C, Strizzi L, Normanno N, Khan N, Salomon DS. Cripto-1: an oncofetal gene with many faces. *Curr Top Dev Biol*. 2005; 67:85–133. [PubMed: 15949532]

**Fig.1.**

GPI-anchored and soluble forms of CR-1. (A) Scheme of TEV-cleavable constructs. (B) Intracellular localization of TEV-cleavable proteins. (C) Activin/Nodal-responsive (n2)7-luciferase assay. Values indicate fold induction of relative luciferase units against EV. Values represent mean \pm SD of three independent experiments. (D) Western blot analysis of TEV-cleaved proteins. Purified TEV-cleavable CR-1 proteins were treated with TEV protease and analyzed by Western blotting with the indicated antibodies. Arrow indicates a COOH-terminal fragment containing GPI moiety after TEV cleavage.

**Fig.2.**

Intercellular transfer of membrane-bound CR-1. (A) Experimental strategy. (B) A representative FACS gating for the Celltracker-negative population (peak A). (C) Cell-surface CR-1 expression in co-cultured 293T cells. CR1WT-transfected 293T cells are shown as a positive control. Peak I: cells co-cultured with EV-transfected 293T cells, peak II: cells co-cultured with CR1WT-transfected 293T cells, peak III and IV: lower and higher peaks for 293T cells transiently transfected with CR1WT, respectively. (D) Cell-surface CR-1 expression in co-cultured 293T cells after PI-PCL treatment. (E) Cell-surface CR-1 expression in co-cultured COS7 cells. Transfected COS7 or 293T cells were used as donors. (F) Cell-surface CR-1 expression in co-cultured 293T cells. CR1TM-transfected 293T cells were used as a donor.

**Fig.3.**

Effect of membrane-forms of CR-1 expression on cellular morphology. (A-B) CR-1 protein was visualized in COS7 cells transiently transfected with the indicated expression vectors. Plasma membrane was stained with wheat germ agglutinin (WGA) in non-permeabilized cells (A) and actin cytoskeleton was visualized with phalloidin in permeabilized cells (B). Arrows indicate sites of cell-to-cell contact by CR-1-induced membrane extensions. (C) Detection of cellular debris/processes on the surface of culture plates (arrows). 293T cells transfected with the indicated expression vectors were grown to subconfluency and photographed with a phase-contrast microscope (large panels) or with a regular light microscope after Hematoxylin-Eosin staining (insets). (D) CR-1 protein localization (green) in 293T cells was assessed three-dimensionally with confocal microscope. Actin cytoskeleton and nuclei were stained with phalloidin (red) and DAPI (blue), respectively. Arrows indicate the adhesion sites at the edge of the cell. (E) Cell adhesion assay of IEC6 clones. Representative images 45 min after seeding are shown in the upper panel. Percentage of flattened cells was manually quantified (lower panel). Values represent mean \pm SD of three independent experiments.